

EDWARD FRAŚ*, ANDRZEJ JANAS*, PAWEŁ KURTYKA**,
STANISŁAW WIERZBIŃSKI**

**STRUCTURE AND PROPERTIES OF CAST Ni₃Al/TiC AND Ni₃Al/TiB₂ COMPOSITES
PART I. SHSB METHOD APPLIED IN FABRICATION OF COMPOSITES BASED
ON INTERMETALLIC PHASE Ni₃Al REINFORCED WITH PARTICLES OF TiC AND TiB₂**

**STRUKTURA I WŁAŚCIWOŚCI KOMPOZYTÓW ODLEWANYCH Ni₃Al/TiC I Ni₃Al/TiB₂
CZEŚĆ I. METODA SHSB WYTWARZANIA KOMPOZYTÓW NA OSNOWIE FAZY
MIĘDZYMETALICZNEJ Ni₃Al WZMACNIANYCH CZĄSTKAMI TiC i TiB₂**

Using SHSB technique, composites "in situ" based on intermetallic phase Ni₃Al reinforced with particles of titanium carbides or borides were fabricated. The reinforcing phase was generated by spontaneous exothermic reaction proceeding in metal bath in a metal/non-metal powdered briquette. Thus fabricated composites were free from porosity, possessed high thermodynamic stability and were characterised by absence of chemical reactions at the matrix-reinforcing particle phase boundary, which effectively prevented structure degradation under high-temperature service conditions. The nucleation of the reinforcing phase in molten metal matrix produced clean interfacial surface, free from the presence of oxides and adsorbed gas, and better wettability and coherence between the matrix and reinforcing particles. Owing to the possibility of controlling the parameters of the reaction kinetics during composite synthesis it was possible to generate particles of a required diameter, volume content and distribution and to obtain, consequently, the required level of the mechanical and tribological properties. An important advantage of this method is the possibility of finally shaping by means of casting process the elements and parts of machines.

In accordance with ANSI H35.1 we use such nomenclature of composite for example Ni₃Al/TiC5p – matrix Ni₃Al, type of reinforcement TiC, vol fraction 5%, p – particles.

Metodą SHSB (Selfpropagating Hightemperature Synthesis in Bath) wytworzono kompozyty „in situ” na osnowie fazy międzymetalicznej Ni₃Al wzmocnionej cząstkami węglików lub borków tytanu, przy czym fazę wzmocniającą wygenerowano w trakcie samorzutnej reakcji egzotermicznej w brykiecie proszkowym metal-niemetal w kąpeli metalowej. Wytworzone kompozyty charakteryzowały się brakiem porowatości, wysoką stabilnością termodynamiczną, jak również brakiem reakcji chemicznych na granicy osnowa – cząstka wzmocniająca, co pozwalało na

* INSTYTUT TECHNOLOGII I MECHANIZACJI ODLEWNICTWA, AKADEMIA GÓRNICZO-HUTNICZA, 30-059 KRAKÓW, AL. MICKIEWICZA 30

** WYDZIAŁ MATEMATYCZNO-FIZYCZNO-TECHNICZNY, AKADEMIA PEDAGOGICZNA, 30-084 KRAKÓW, UL. PODCHORAŻYCH 2

wyeliminowanie degradacji struktury w warunkach wysokotemperaturowej eksploatacji. Zarodkowanie fazy wzmacniającej w kąpeli osnowy zapewnia czystą powierzchnię międzyfazową pozbawioną tlenków i zaadsorbowanych gazów, a także lepszą zwilżalność i spójność osnowy z cząstkami wzmacniającymi. Możliwość sterowania parametrami kinetyki reakcji w procesie syntezy kompozytów pozwala na generowanie cząstek o pożądanej średnicy, udziale objętościowym i rozkładzie, co w konsekwencji determinuje poziom właściwości mechanicznych i trybologicznych. Ważną zaletą tej metody jest możliwość nadawania finalnego kształtu detalom i częściom maszyn metodami odlewniczymi.

1. Introduction

Metal matrix composites are considered to be constructional materials with a wide spectrum of applications within the field of advanced technique, and as such since many years now they have been the main object of interest of numerous research and development centres. Among various composite materials, particular interest raises the group of composites "in situ", in which the reinforcing phases are formed as a consequence of reactions proceeding in the liquid metal matrix directly during the metallurgical process. Usually, for the matrix of metal composites are used metals, like aluminium, magnesium, titanium, cobalt, copper, or their respective alloys, while the reinforcing phase are high-melting point, hard particles of ceramic compounds, like carbides, borides and nitrides of titanium, hafnium, vanadium, tungsten, molybdenum and niobium.

This study describes the process of fabrication of new composite materials in which the matrix has been formed of an intermetallic compound Ni_3Al , and the reinforcing phase is titanium carbide or boride of high-melting point, generated by the method of self-propagating, exothermic reaction of synthesis in metal bath (SHSB) [1]. The criteria used in selecting an alloy for the composite matrix were based, first of all, on an optimum strength-to-density ratio (R_m/γ), the stability of mechanical properties at high temperatures and resistance to the effect of chemical agents, mainly diluted acids and waste gas [2–5]. A serious restriction in the applicability range of intermetallic compounds in industry is their limited plastic deformability and brittleness at ambient temperature, both of which can be, at least partially, improved by the use of microadditives of metals like Nb, Zr or Hf [6]. In the examined composites the mechanical properties of the base alloy were improved by introducing boron as a microadditive to the intermetallic compound of Ni_3Al .

2. Theoretical backgrounds of Ni_3Al/TiC and Ni_3Al/TiB_2 composites fabrication

Composites "in situ" are generally considered the materials of the second generation [7]. Contrary to composites "ex situ", they are characterised by high thermodynamic stability which effectively counteracts the occurrence of chemical reactions at the matrix-reinforcing particle phase boundary, reducing structure degradation during service at high temperatures. The nucleation of a reinforcing phase in the liquid matrix provides clean surface of the interface and, consequently, better wettability. The interface surfaces are resistant to oxidation and gas adsorption which, in turn, improves the cohesion between the

matrix and reinforcing particles. The possibility of controlling the dimensions of the reinforcing particles through changes in the parameters of the kinetics of the reaction of composite synthesis enables generating particles of very small dimensions and, as a consequence, increases the composite reinforcement.

Among numerous methods of the synthesis of TiC in liquid aluminium or its alloys, special attention deserves the technique of RGI (Reactive Gas Injection), utilising a reaction at the solid body -gas phase boundary [8]. In this method, the aluminium-titanium alloy melt is blown with methane. In another process, utilising a reaction proceeding in the solid body -liquid body system, carbon is obtained from the decomposition of silicon carbide in liquid aluminium-titanium alloy [9]. The liberated carbon enters into reaction with titanium, forming a finely-dispersed phase of TiC. The next method is based on a reaction proceeding in the solid body-solid body system, and it was developed by Martin Marietta Corporation (XDTM) [10]. The method consists in mixing metallic and non-metallic powders, followed by preheating of the obtained mixture to a temperature above the pure metal melting point. Detailed specification of this technique is protected by a patent.

In the process of composite synthesis “in situ” the most important are the reactions of the formation of carbides, nitrides and borides of elements such as titanium, zirconium and hafnium; the carbides are in this case acting as particles reinforcing the matrix. Since the melting points of most of the carbides, nitrides and borides are relatively high, producing of these compounds, important for numerous sectors of industry, is possible by reactions proceeding in the solid phase. According to the results of investigation made by Tamman [11], a reaction between the solid bodies can occur upon heating them when they remain in direct contact with each other, without the need of an intervention of the liquid or gaseous phase. Numerous reactions take place in the solid phases at temperatures lying much below the melting point of either the reagents or the eutectics which can be formed thereof. In the case of oxides being formed from solid substrates, the temperatures of reaction are comprised within a range in which the gaseous phase cannot be formed any longer by the decomposition of reagents or their evaporation, since the process is proceeding under isothermal conditions. During the reaction a solid solution is not formed, neither is the state of equilibrium achieved by the system, and therefore the reaction is proceeding in certain direction until the moment when one of the reagents is exhausted completely.

Quite a different course assumes the reaction of synthesis of titanium carbides, borides or nitrides. After mixing the powdered titanium with carbon and local preheating, the reaction between the solid components starts below the melting point of the reagents, but its exothermic character liberates large amounts of the thermal energy (the adiabatic process), which increases the temperature up to about 5000 K. The forming liquid titanium phase enables rapid propagation of SHS reaction (Self Propagating High Temperature Synthesis) [12], which lasts until the reagents are completely exhausted, with energy produced in an amount of 180 kJ/mole.

Schematically, the reaction between two solid bodies resulting in formation of a new chemical compound in the solid phase can be described as :



Every reaction proceeding in the presence of solid phases is a combination of several partial processes, like proper chemical reactions, the process of mass and heat transfer, and processes related with changes in the state of aggregation, and therefore the kinetics of reaction is a function of all these factors. To describe the process of titanium carbide synthesis, some simplifications have been adopted, and the reaction was divided into several stages considered at both micro- and macroscopic levels. At a micro-level, the first stage starts with thorough mixing and pressing of powdered titanium and carbon to ensure mutual contact between the grains of the reagents. Due to thermal vibrations, at the places where the grains are touching each other, the individual atoms of the first reagent enter the zone where the forces of the crystal lattice of the second reagent are acting and make atoms of the first reagent get adsorbed to the surface of the second reagent. At the second stage, thus adsorbed particles, remaining under the effect of forces which are acting at the phase boundary, continue to be very active, and this activity increases with the increase of temperature.

At the third stage, the monomolecular layer of a more mobile element (titanium) covers locally (at selected points) the surface of the crystal of another element (carbon or boron), forming particles loosely combined with each other, mobile and very active. At the fourth stage, further increase of temperature makes titanium pass into liquid state, and it is then when a thin layer of the liquid titanium encloses the grains of carbon or boron, causing interdiffusion of the constituents and change in the parameters of the crystal lattice of the element in which the diffusion and further increase of activity take place. The rate of the reaction of synthesis of titanium carbide is also increasing. At the next stage, the number of the particles of the TiC or TiB₂ phases which can diffuse inside alien crystals is limited, because of the formation of aggregates of the TiC or TiB₂ crystals, which enter the metal matrix forced there by, e.g., the SHSB process.

According to the model developed by Komatsu [13], the main role in the reaction between the solid bodies (titanium-carbon, titanium-boron) plays the number of intergranular contact points, which depends on a ratio between the number and size of the radii of the grains of both constituents, in other words, on the composition of the system. In a model assuming the spherical shape of reacting particles, the number of contact points between particle *A* and the neighbouring particles *B* is determined by [14]:

$$n(A/B) = n_0 \left(\frac{ab}{1 + ab} \right)^m, \quad (2)$$

where: n_0 – total number of particles *A* and *B* surrounding the examined particle, b – element *B*-to-element *A* content ratio in the system expressed in kg, a – single particle *A*-to-single particle *B* mass ratio, m – parameter accounting for differences in packing degree resulting from different sizes of the radii of the reacting particles.

Assuming that the relationship between the number of contact points and time equals:

$$n(t) = n(A/B) \left(1 + g \left(\frac{t}{t_f} \right)^t \right), \quad (3)$$

where: t – time in which $n(t)$ reaches its maximum equal to $n(A/B)(1 + g)$, and the rate of reaction is directly proportional to the number of contact points $n(A/B)$ and inversely proportional to the thickness of the layer of reaction product, while g and l are material parameters, this rate can be expressed by formula which results from the Fick's first law:

$$\frac{dy}{dt} = kn(A/B) \frac{1}{y}, \quad (4)$$

where: y – thickness of the layer of reaction product, and $\frac{dy}{dt}$ the rate of the reaction product transfer. After integration:

$$y^2 = 2kn(A/B)F(t, t^{+1}), \quad (5)$$

where: k – function of temperature and of the number of contact points hence:

$$k(T, a, b) = k_0(T) \left(\frac{ab}{1 + ab} \right)^m \quad (6)$$

and the obtained result proves that constant k is function of temperature, of the ratio of the size of the radii of the particles of both constituents (parameter a), and of the ratio of the content of both constituents in a system (parameter b). It is worth noting that the quantity (y^2) expresses a relative amount of the substrate (x) which has been formed as a result of the reaction proceeding according to equation:

$$x = \frac{\frac{4}{3}\pi r_0^3 - \frac{4}{3}\pi(r_0 - y)^3}{\frac{4}{3}\pi r_0^3}, \quad (7)$$

where: r_0 – starting radius of the constituent particles, $(r_0 - y)$ – the radius of particles after the lapse of time t , (y) – implicit function (x).

The process of pressing makes the number of the intergranular contact points in a reacting mixture raise, and with appropriate disintegration and mass (volume) fraction of the constituents it is possible to create proper conditions for an effective control of the reaction of synthesis.

To describe the course of a typical SHS reaction, a simple thermodynamic model was used. It has been assumed that under given conditions the exothermic reaction is initiated by heat Q_z , supplied to the system from the outside, and typically produces heat Q_w . Since perfect heat insulation is not possible, the energy is dissipated in the form of heat Q_o . Under the conditions of SHS process, the rate of heat evolution is higher than the rate of heat transfer:

$$Q_w > Q_o \quad (8)$$

hence the energy is accumulated, resulting in an increase of temperature. In the case of the thermally activated reactions, the increase of temperature moves the rate of reaction to a higher level, and hence also the rate of the evolution of thermal energy. This positive feedback acts as an “ignition” to the self-propagating reaction of synthesis, which is going on until the individual reagents are completely exhausted. The degree of this feedback is determined by a relationship which has been reported to exist between the rate of reaction and temperature which, for chemical reasons, are determined by Arrhenius equation. The reaction of synthesis depends on the energy of activation, and higher energy of activation means better self-heating capacity of the thermodynamic system. This is why the process running under the nearly-adiabatic conditions is most desired.

Figure 1 shows the principle of the titanium carbide synthesis by SHS process. Upon preheating, e.g. the upper surface of a sample (a briquette) which is a mixture of the pressed powders of Ti and C, a strong exothermic reaction starts. Inside the material the front of this reaction is moving forward at a rate u , leaving behind the TiC carbides which have already undergone the process of synthesis.

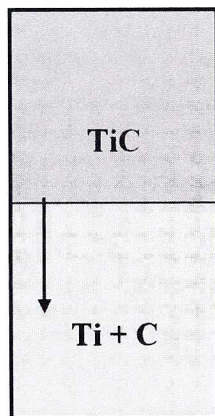


Fig. 1. Schematic representation of the SHS process

The synthesis by the SHS process is possible when the proceeding reaction is of a strongly exothermic character with the heat of reaction amounting to -170 kJ/mole. In the case of reaction of titanium carbides synthesis, the evolving heat of reaction amounts to -185 kJ/mole [15], which means that the amount of thermal energy transferred to the unreacted volume of material is sufficient to make the temperature increase.

Figure 2 shows the distribution of temperature, the volume fraction of reaction product, and the rate of heat generation during the synthesis of TiC by SHS. It has been established that the product of reaction must be in liquid or gaseous form to serve as a medium in which, due to the effect of diffusion, the individual elements of an alloy or a mixture of these elements will be transported. The rate of transport (by conduction or radiation) of the heat generated

by exothermic reaction should be lower than the rate at which this heat is generated by this reaction, otherwise the reaction will be extinguished.

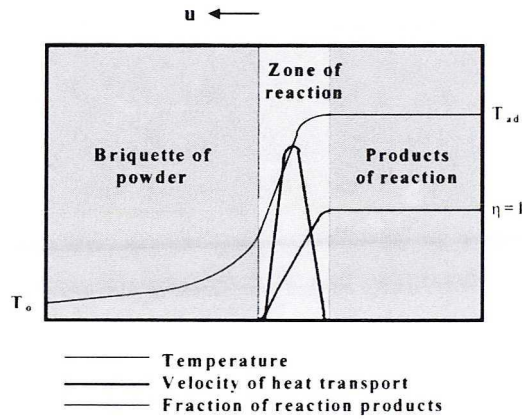


Fig. 2. Temperature distribution, content of reaction products, and heat generation rate during the SHS synthesis

The synthesis of materials by the SHS process is accompanied by a high temperature of reaction, reaching even 5000 K, and also by a high rate of transfer of the reaction front, reaching 0,25m/s and with the thermal gradient of 10^7 K/m.

One of the important parameters of the SHS process is the adiabatic temperature T_{ad} , determining the maximum temperature which can be locally reached by the product of reaction under the assumed conditions of total lack of the heat losses to environment.

For reaction:



where: M , X and MX – metal, non-metal and products of synthesis in solid state (e.g. carbide), respectively.

The adiabatic temperature can be calculated as a function of the upper limit of integration from relationship [15]:

$$\Delta H_{T_0}^0 = \int_{T_0}^{T_{ad}} c_m(MX) dT, \quad (10)$$

where: $\Delta H_{T_0}^0$ – the enthalpy of formation of compound MX at a temperature T_0 , $c_m(MX)$ – molar heat of reaction product.

The synthesis of titanium carbide proceeds at $T_{ad} = 3210$ K [15]; that of titanium boride at $T_{ad} = 3400$ K [16]. In practice, the thermodynamic system never can reach this temperature and the actual temperature of reaction is much lower than T_{ad} , which is due to the dissipation of heat to the system in which the process is going on as well as its consumption needed for the formation of new phases.

In a ternary system of aluminium, titanium and carbon, or aluminium, titanium and boron, numerous chemical reactions are possible between either both alloy constituents or between the phases formed in the alloy. Nickel, as an element resistant to reaction with carbon, has been disregarded in these equations. In the case under discussion, the following reactions are most important:



Because application of the SHS process of synthesis could not guarantee fabrication of the entirely pore-free products, and the high volume fraction of the ceramic compounds present after the synthesis made shaping of products to the desired final configuration difficult, a modified variation of the process of composite fabrication “in situ” was developed. This is the SHSB process, schematically drawn in Figure 3. The essence of the SHSB process consists in the fact that instead of initiating the reaction by supply of the heat from an external source, the briquette of powdered material is placed directly on the surface of liquid metal in a crucible of induction furnace. The melt is then acting as a system “cooling” the exothermic reaction and also as a “diluent”, while its stirring (by electrodynamic force) causes erosion of the briquette and distribution of reaction products (the reinforcing phase) in the melt.

Simple calculations resulting from the law of energy conservation indicate that in the SHSB process the temperature of the liquid metal is not increasing very dramatically and is much lower than T_{ad} . Assuming now that the heat Q_s evolved during the reaction of TiC synthesis equals the heat Q_m transferred to the metal melt, it is possible to determine the melt temperature after the exothermic reaction using relationship:

$$T_k = T_0 + \frac{Q_s}{m \cdot c}, \quad (15)$$

where: T_0 – initial temperature before the exothermic reaction, c – specific heat of aluminium at a temperature of 1500 K, m – mass of suspension.

It has been the aim of the described SHSB method of synthesis to create a simple thermodynamic system with possibly small number of the degrees of freedom. Therefore it has been decided to use in the synthesis pure constituents, i.e. Ni, Al, Ti and C or B.

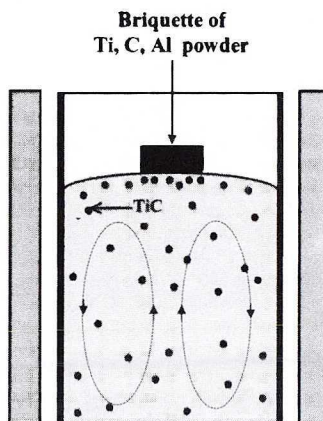


Fig. 3. Schematic representation of the SHSB synthesis of metal matrix composites reinforced with ceramic particles

The volume fraction of the reinforcing phase produced in the form of titanium carbide particles was reported to be dependent on the amount of powdered briquettes introduced to the melt, where the size of titanium carbide or boride particles was function of the time during which the system remained in liquid state until the moment when the SHSB reaction had been completed. The structure of thus produced composite depends on the weight of the introduced briquettes, which is related with the originally assumed volume content of the reinforcing phase, the time of synthesis affecting the dimensions of the titanium carbide particles, and the temperature on which the reaction of “ignition” depends as well as on the possible presence of an aluminium carbide phase.

3. The cost-effective melting process (OPW)

The specific nature of the process of formation of an intermetallic Ni_3Al phase results from large differences in the melting points of aluminium and nickel and from the presence of exothermic reaction accompanying the synthesis of intermetallic alloys, which determines the way in which the metallurgical process is conducted. Due to the rapid increase of temperature up to 1600 K, immediately after the exothermic reaction between aluminium and nickel has been completed in the atmosphere, aluminium gets oxidised with abundant slag formation, making precise control of alloy composition difficult. In practice, different melting techniques are used, mainly in open induction furnace, in vacuum furnace, or in vacuum arc furnace [5, 16]. The Ni-Al (Ni_3Al) alloy was also melted in argon atmosphere, applying the negative gas pressure of 0.5 MPa, the power of 5 kW and the time of 500 sec (counting from an instant of switching the furnace on until pouring). Charging of furnace for the OPW process is schematically drawn in Figure 4.

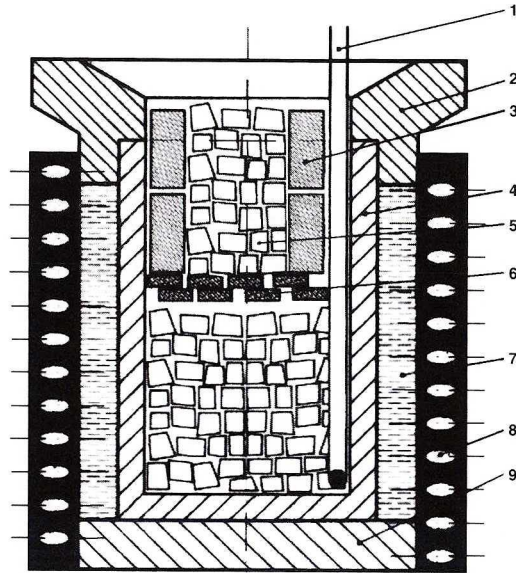


Fig. 4. Procedure of crucible charging (Exo-Melt™ process [17]), 1 – Pt-Pt 18Rh thermocouple; 2 – graphite top coated with Morgan cement; 3 – aluminium; 4 – ceramic (Al_2O_3) crucible; 5 – nickel; 6 – alloying elements (Al-B master alloy); 7 – spinel composition ($\text{Al}_2\text{O}_3\text{MgOZrO}_2$); 8 – induction coil; 9 – ceramic base (Al_2O_3)

With constant power of 5 kW fed to the induction furnace and maintaining the angle of phase displacement constant, the energy required for preheating and melting down of the charge depends on the process duration, counting from the moment when the power is switched on until the moment of mould pouring. The duration of the OPW process counting from the moment when the coil of induction furnace starts working until the moment when the required pouring temperature of 1780 K has been reached is 500 sec., while the time of a common melting process is 820 sec, including preheating and melting of pure nickel, with the temperature of 1780 K reached, also aluminium. Compared with the common melting process, the effectiveness of the OPW process with the power value kept constant can be expressed by ratio η of the process duration:

$$\eta = \frac{t_1}{t_2} 100\% = 60\% \quad (16)$$

which gives 40% savings in electric energy consumption. The exothermic reaction of Ni-Al takes several seconds; after it has been completed the alloy is ready for pouring by any common method into a mould, which in this particular case is a preheated metal mould and/or ceramic mould. Using this method, the following materials were produced: Ni_3Al phase characterised by a composition consistent with the law of stoichiometry, NiAlB alloys with different boron content levels, and Ni_3AlTiC and $\text{Ni}_3\text{AlTiB}_2$ composites.

5. Examinations of Ni₃Al phase structure

To evaluate the structure of material before and after introducing boron microadditives in an amount of 0.05 wt.% B, the diffraction patterns obtained on samples taken before and after the process of yielding the Ni₃Al phase were used. The results are shown in Figures 5 and 6, which reveal no major changes in arrangement of diffraction reflexes before and after boron has been added as a microadditive.

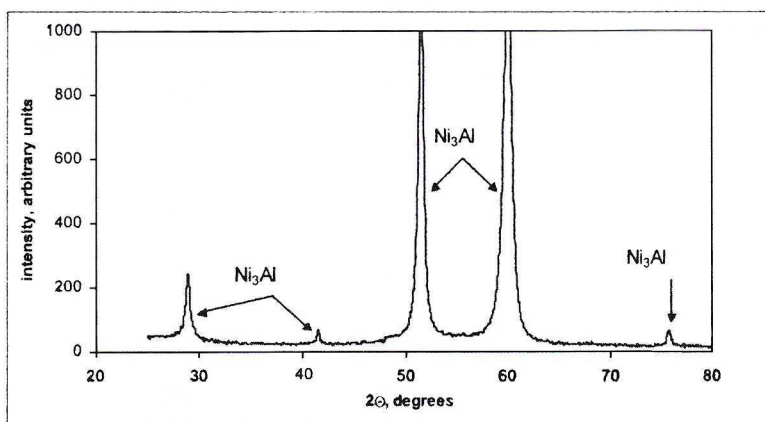


Fig. 5. Diffraction pattern of boron-free Ni₃Al phase

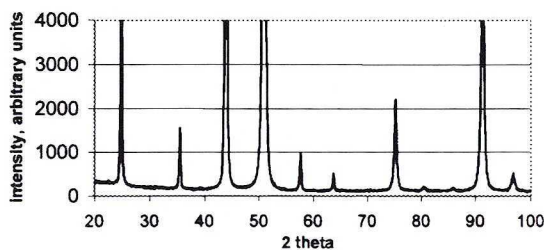


Fig. 6. Diffraction pattern of Ni₃Al phase containing 0.05% boron

The effect of boron microadditives (0; 0.002; 0.01; 0.05; 0.2 wt.%) on changes of the crystal lattice parameters of Ni₃Al phase was examined, too. The average value of parameter *a* was 0.35666 nm, the mean relative error σ was at a level of 0.15%. This, very small, measuring error proves the lack of an effect of boron microadditive on the size of an elementary cell of the Ni₃Al phase. The weight percent content of the individual matrix constituents was given in Table 1.

The weight percent content of the individual matrix constituents

Ni ₃ Al + 0.05% B matrix			
Matrix composition	Ni	Al total	AIB3 master alloy
Content [g]	575.00	76.80	11.00

Observations of composite matrix under the microscope were made on specimens cast in a die and in a ceramic mould. The fracture of the cast bars is shown in Figures 7 and 8. Radially oriented columnar grains are visible.

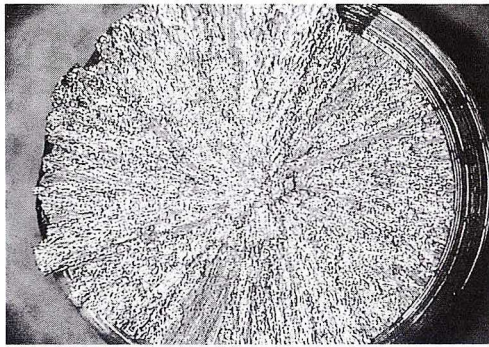


Fig. 7. Die cast bar cross-section. Magnification 10x

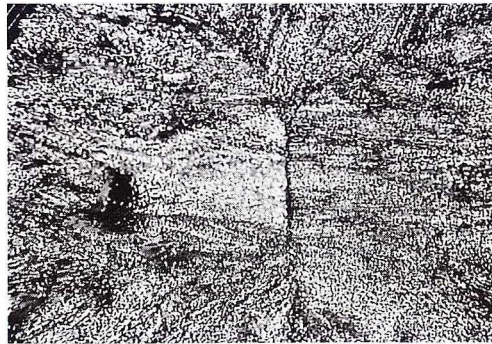


Fig. 8. Die cast bar cross-section. Magnification 50x

In the same place on the cross-section SEM photographs were taken (Fig. 9). On all the photographs are visible structural discontinuities located near the bar axis. The discontinuity in the form of a slot, running along the bar axis, has been caused by an excessive casting shrinkage and too rapid cooling process. To eliminate these defects, a series of ceramic moulds was made using molochite flour hardened with sodium silicate.



Fig. 9. SEM image of fracture of the die cast $\text{Ni}_3\text{Al} + 0.05\% \text{B}$ material, 200x

The microstructures of castings made in ceramic moulds were free from the defects in the form of cracks and discontinuities on grain boundaries. The grains with well visible dendrites had the dimensions of 1–5 mm. (Figs. 10, 11 and 12)

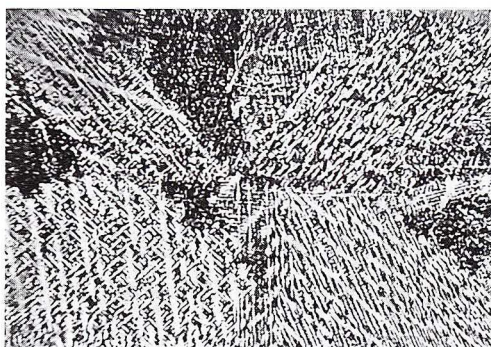


Fig. 10. Microstructure of Ni_3Al phase in test bar before yielding, 15x

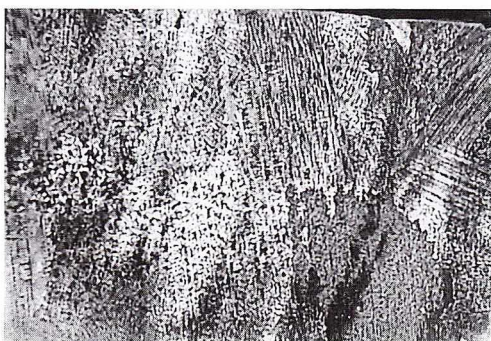


Fig. 11. Microstructure of Ni_3Al phase in test bar after yielding with an addition of 0.05 wt.% boron, 15x

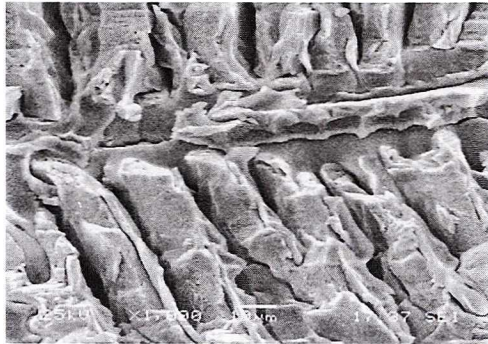


Fig. 12. Fracture of the yielded Ni_3Al phase running along the plane parallel to dendrite axis, 1000x

6. The SHSB synthesis of titanium carbide in liquid phase of Ni_3Al

The starting material for the synthesis of titanium carbide in Ni_3Al phase were charges of Ni, Al and AlB master alloy which were pressed under a pressure of 500 MPa, conferring to them the shape of Ti-Al-C briquettes of compositions given in Tables 2 and 3.

TABLE 2

Starting materials for synthesis of $\text{Ni}_3\text{Al}/\text{TiC}/5\text{p}$ composite

$\text{Ni}_3\text{Al} + 0.05\% \text{ B} + 5\% \text{ TiC}$ composite			
Matrix composition	Ti	Al total	AlB3 master alloy
Content in matrix [g]	575.00	76.80	11.00
Briquette weight [g]	33.00 including 22.00 g TiC		
Grain size of powdered Ti, Al, C – approx. 40 μm			
Charge (matrix) volume [cm^3]	90.00		
Reinforcing phase volume, TiC [cm^3]	4.50		
Percent fraction of reinforcing phase, TiC [vol.%]	5.0		

With Exo-Melt reaction in OPW process completed, the briquettes of powdered Ti, C and Al were immersed in liquid metal at a temperature of about 1700 K, which initiated the reaction of titanium carbide synthesis. The produced by SHS synthesis, particles of titanium carbide were distributed in the melt due to the movement of liquid metal induced by induction stirring. With the reaction of synthesis completed, the metal was held in the crucible of a vacuum furnace under the protective atmosphere of argon at a temperature of

TABLE 3

Starting materials for synthesis of Ni₃Al/TiC/10p composite

Ni ₃ Al + 0.05% B + 10% TiC composite			
Matrix composition	Ti	Al total	AlB3 master alloy
Content in matrix [g]	575.00	76.80	11.00
Briquette weight [g]	66.00 including 44.00 g TiC		
Grain size of powdered Ti, Al, C – approx. 40 μm			
Charge (matrix) volume [cm ³]	90.00		
Reinforcing phase volume, TiC [cm ³]	9.00		
Percent fraction of reinforcing phase, TiC [vol.%]	10.0		

With Exo-Melt reaction in OPW process completed, the briquettes of powdered Ti, C and Al were immersed in liquid metal at a temperature of about 1700 K, which initiated the reaction of titanium carbide synthesis. The, produced by SHS synthesis, particles of titanium carbide were distributed in the melt due to the movement of liquid metal induced by induction stirring. With the reaction of synthesis completed, the metal was held in the crucible of a vacuum furnace under the protective atmosphere of argon at a temperature of 1700 K for 5 minutes, to be next cast into a ceramic mould where it solidified as a composite material.

7. The structure of Ni₃Al/TiC composite

The structure of Ni₃Al/TiC/5p composite material is shown in Figures 13, 14 and 15.

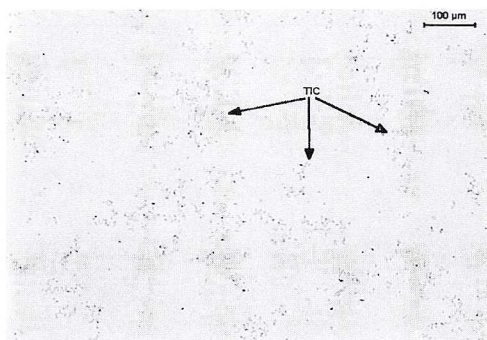


Fig. 13. Microstructure on composite surface (Ni₃Al/TiC/5p). Note titanium carbide precipitates visible in the interdendritic spaces, 100x



Fig. 14. A topographic image of the shape and size of titanium carbide precipitates in Ni₃Al/TiC/5p composite material, 500x

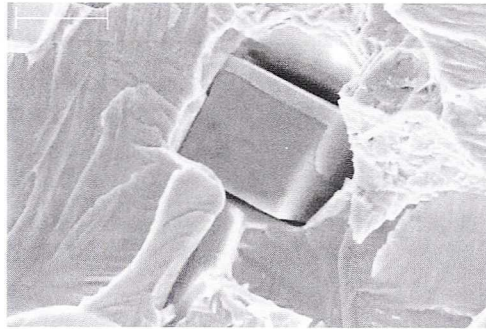


Fig. 15. Cubic precipitates of titanium of carbide (10–15 μ m) visible on the fracture of a tensile specimen of Ni₃Al/TiC/5p composite material

The phase constitution of Ni₃Al/TiC composite material containing 5 and 10 vol.% of TiC was evaluated from diffraction patterns shown in Figures 16 and 17. On these diffraction patterns some reflexes coming from TiC phase are visible against the reflexes typical of Ni₃Al phase.

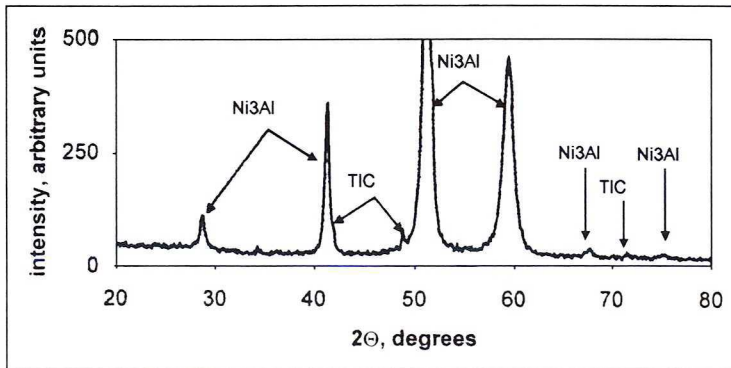


Fig. 16. Diffraction pattern of Ni₃Al/TiC/5p composite material. Note reflexes visible from TiC phase

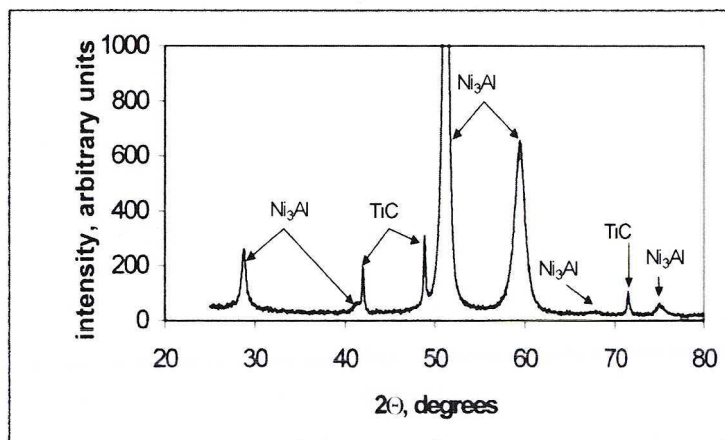


Fig. 17. Diffraction pattern of Ni₃Al/TiC/10p composite material

The X-ray structure examinations also provided information on the type and magnitude of parameters of the crystal lattice in both matrix and reinforcing phase of the composite (Table 4). Basing on the results of the quantitative metallography and X-ray microanalysis, the volume content and chemical composition of the reinforcing phase and composite matrix were determined.

TABLE 4
Structure types, lattice parameters and volume content of the matrix and reinforcing phase

	Type of structure	Lattice parameters	Volume content	Chemical composition
Ni ₃ Al + 0.05%B	L1 ₂ , regular orientation Pm3m	0.3513–0.570 ± 0.0002 nm (theoret. 0.3572 nm) [21]	95.0% and 90.0%	Ni – 86.5 ± 2% Al – 13.5 ± 3% B – 0.05 vol.%
TiC 5%	A1, F m3m orientation	0.4319 – 0.4331 ± 0.0002 nm (theoret. 0.4327 nm) [21]	4.8 ± 0.4 (theoret. 5.0%)	Ti – 79.8 ± 0.2 wt.% C – 20.0 ± 0.3 wt.%
TiC 10%	as above	as above	9.6 ± 0.5 (theoret. 0.0%)	Ti – 79.7 ± 0.2 wt.% C – 20.0 ± 0.3 wt.%

The results compiled in Table 4 show a consistency obtained between the assumed volume content and stoichiometric composition of the reinforcing phase and composite matrix; the types of structure are consistent with data compiled in the table. No presence of aluminium carbide, affecting in an unfavorable way the utilisation properties of composites, was traced in the structure of Ni₃Al/TiC composite.

8. The SHSB synthesis of titanium boride in liquid phase of Ni₃Al

Charges of Ni and Al with AlB master alloy were prepared and briquettes of Ti-Al-B of the compositions given in Tables 5 and 6 were pressed under a pressure of 500 MPa.

TABLE 5
Starting materials for synthesis of Ni₃Al/TiB₂/5p composite

Ni ₃ Al + 0.05% B + 5% TiB ₂ composite			
Matrix composition	Ti	Al total	AlB3 master alloy
Content in matrix [g]	575.00	76.80	11.00
Briquette composition [g]	Ti	B	Al
	14.00	6.34	10.00
Briquette weight [g]	30.34 including 20.24 g TiB ₂		
Grain size of powdered Ti, Al, B – approx. 40 μm			
Charge (matrix) volume [cm ³]	90.00		
Reinforcing phase volume, TiB ₂ [cm ³]	4.50		
Percent fraction of reinforcing phase, TiB ₂ [vol.%]	5.0		

TABLE 6
Starting materials for synthesis of Ni₃Al/TiB₂/10p composite

Ni ₃ Al + 0.05% B + 10% TiB ₂ composite			
Matrix composition	Ti	Al total	AlB3 master alloy
Content in matrix [g]	575.00	76.80	11.00
Briquette composition [g]	Ti	B	Al
	28.00	12.68	20.34
Briquette weight [g]	40.68 including 20.34 g TiB ₂		
Grain size of powdered Ti, Al, B – approx. 40 μm			
Charge (matrix) volume [cm ³]	90.00		
Reinforcing phase volume, TiB ₂ [cm ³]	9.0		
Percent fraction of reinforcing phase, TiB ₂ [vol.%]	10.0		

With Exo-Melt reaction in OPW process completed, the briquettes of powdered Ti, Al and B were immersed in liquid metal at a temperature of about 1700 K, which initiated the reaction of titanium boride synthesis. The synthesis of Ni₃Al/TiB₂ composite is schematically shown in Figure 18.

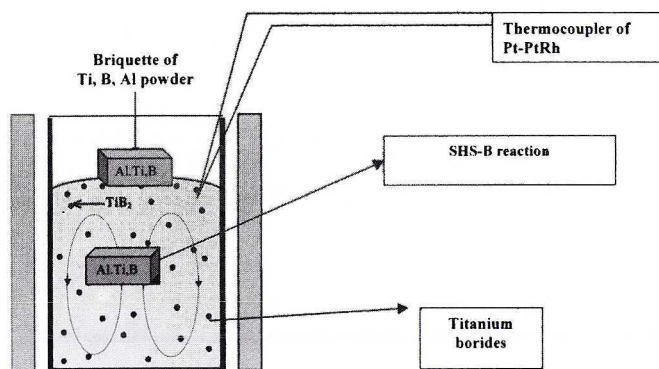


Fig. 18. Schematic representation of SHSB synthesis of titanium boride in melt with liquid Ni_3Al phase

With the reaction of synthesis completed, the metal was held in the crucible of a vacuum furnace under the protective atmosphere of argon at a temperature of 1700 K for 5 minutes, to be next cast into a ceramic mould where it solidified as a composite material.

9. The structure of $\text{Ni}_3\text{Al}/\text{TiB}_2$ composite

The structure of $\text{Ni}_3\text{Al}/\text{TiB}_2/5\text{p}$ composite material is shown in Figures 19 and 20. Fine precipitates of titanium boride are distributed in a uniform manner within the matrix volume. The precipitates of titanium boride are characterised by blurred phase boundaries. To X-ray for microanalysis the precipitates of so small dimensions was both difficult to perform and gave ambiguous results, mainly because the precipitates contained boron, i.e. an element difficult to discern in microregions by the technique of X-ray spectroscopy. An additional obstacle in this microanalysis were small dimensions of the precipitates ($5\mu\text{m}$), comparable with the resolution power of a microanalyser.

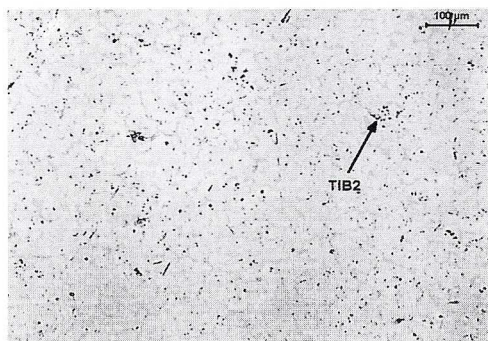


Fig. 19. Microstructure on the surface of $\text{Ni}_3\text{Al}/\text{TiB}_2/5\text{p}$ composite. Note well visible precipitates of titanium borides, 100x

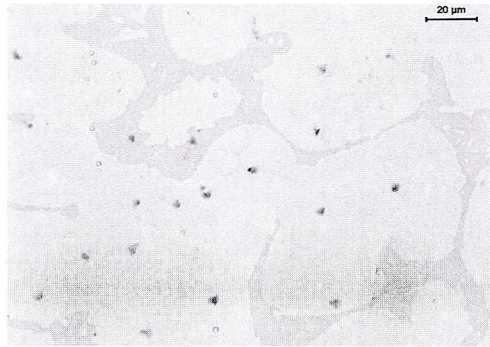


Fig. 20. Microstructure on the surface of Ni₃Al/TiB₂/5p composite, 500x

In the light of a SEM image these precipitates are hardly distinguishable from the matrix. As a result of exothermic reaction proceeding in alloy melt with the added boron-containing briquettes, the structure of the matrix changed, too. A nickel-rich phase appeared (Fig. 20 – dark phase). At the same time, the presence of titanium in the chemical composition of the matrix was noted. The results of examinations of the chemical composition of the matrix are given in Table 7.

TABLE 7

Chemical composition of the matrix

Type of phase	Examined element	Content [wt. %]
Light phase	Ni	85.0
	Ti	1.6
	Al	13.4
Dark phase	Ni	92.0
	Ti	0.6
	Al	7.4

In the case of Ni₃Al/TiB₂/5p composite, the precipitates of titanium boride can be identified from the results of an X-ray diffraction analysis. A diffraction pattern of this composite is shown in Figure 21.

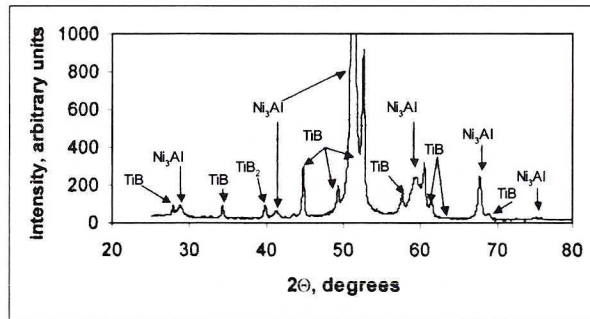


Fig. 21. Diffraction pattern of Ni₃Al/TiB₂/5p composite material. Note strong reflexes visible from the precipitates of titanium borides

The X-ray diffraction analysis revealed the presence in the composite of two types of titanium borides, viz. TiB and TiB₂. The scanning image of the fracture of a composite specimen (Fig. 22) shows the morphology of titanium boride precipitates.

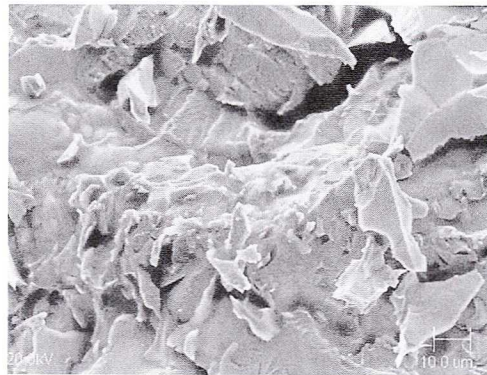


Fig. 22. Precipitates of titanium borides visible on the fracture of Ni₃Al/(TiB, TiB₂)/5p composite specimen after the tensile test

In the photograph are visible the precipitates of irregular crystal boundaries which have been suffering additional destruction during the tensile rupture. Similar examinations were carried out for Ni₃Al/(TiB, TiB₂)/10p composite. Like in the case of Ni₃Al/TiB, TiB₂/5p composite, also here the matrix is composed of two phases. Compared with the shape of titanium carbide and titanium boride precipitates in Ni₃Al/TiB, TiB₂/5p composite, the shape of titanium boride crystals is quite different (Fig. 23). In Ni₃Al/(TiB, TiB₂)/10p composite, borides are present in the form of oblong needles, combined into regular skeletons, distributed within the entire volume of material (Figs 24, 25 and 26).

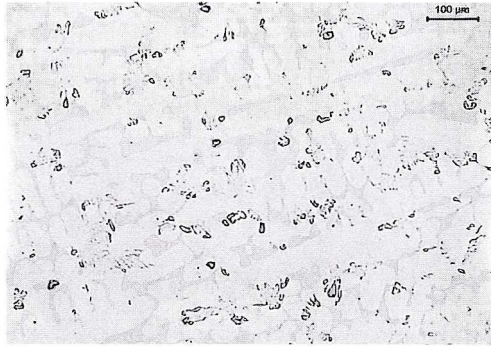


Fig. 23. Microstructure on the surface of Ni3Al/(TiB,TiB2)/10p composite. Note well visible precipitates of titanium borides, 100x

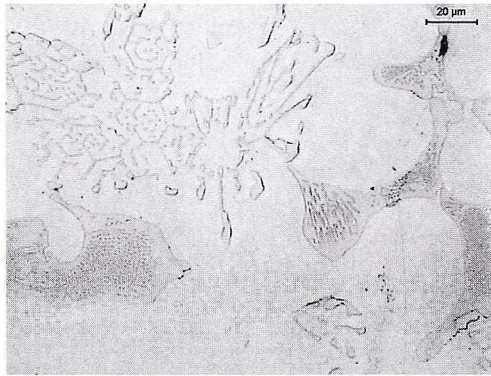


Fig. 24. Microstructure on the surface of Ni3Al/(TiB,TiB2)/10p composite. Note well visible precipitates of titanium borides, 500x

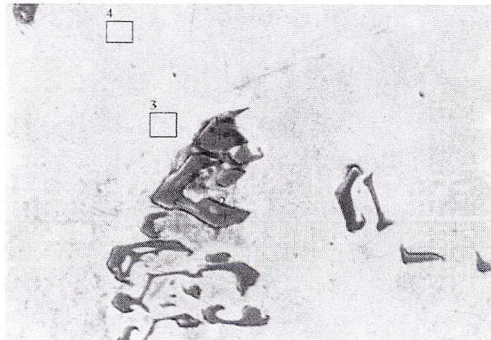


Fig. 25. A topographic image of titanium carbide precipitates in Ni3Al/(TiB,TiB2)/10p composite, 500x

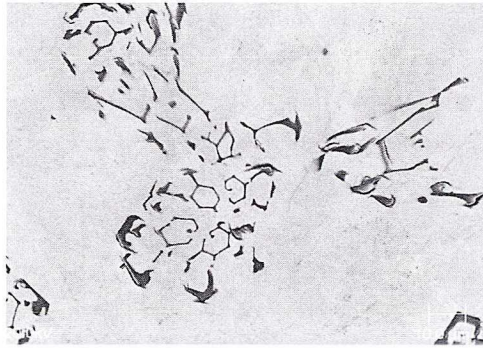


Fig. 26. A topographic image of titanium carbide precipitates in Ni₃Al/(TiB,TiB₂)/10p composite, 1000x

To identify the individual phases, an X-ray microanalysis of borides and of the matrix was carried out; its results are compiled in Table 8.

TABLE 8
Results of an X-ray microanalysis of the individual phases in Ni₃Al/(TiB,TiB₂)/10p composite

Type of phase	Examined element	Content [wt. %]
Borides	B	53.30
	Al	0.02
	Ti	45.00
	Ni	1.60
Light phase in matrix	B	0.00
	Al	13.60
	Ti	1.55
	Ni	84.80
Dark phase in matrix	B	0.00
	Al	8.50
	Ti	2.00
	Ni	89.50

As the case of Ni₃Al/(TiB,TiB₂)/5p composite, the composition of both matrix was far from a stoichiometric system. A relevant graph plotted from an X-ray diffraction pattern is shown in Figure 27. Similar as in the case of Ni₃Al/(TiB,TiB₂)/5p composite, the presence of two types of titanium borides, i.e. TiB and TiB₂, was stated. A SEM image of the fracture

of composite specimen (Fig.28) shows the morphology of titanium boride precipitates in Ni₃Al/(TiB,TiB₂)/10p composite.

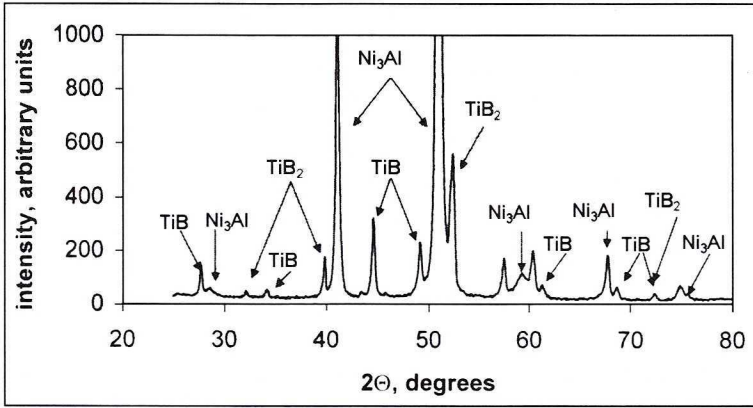


Fig. 27. Diffraction pattern of Ni₃Al/(TiB,TiB₂)/10p composite material. Note reflexes visible from the precipitates of titanium borides

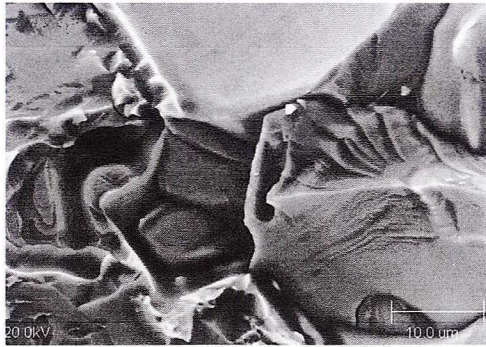


Fig. 28. Precipitates of titanium borides (central part of the image) visible on the fracture of Ni₃Al/(TiB,TiB₂)/10p composite specimen after the tensile test

As in the case of Ni₃Al/TiC composite, the X-ray structure examinations provided information on the type and value of the crystal lattice parameters in both matrix and reinforcing phase of the composite. For titanium borides the obtained results are less ambiguous than in the case of the identified titanium carbide phase. The examinations made by the quantitative metallography and X-ray microanalysis also enabled the volume content of the reinforcing phase to be determined. The values of these parameters are compiled in Table 9.

TABLE 9

Structure types, lattice parameters and volume content of the matrix and reinforcing phase

	Type of structure	Lattice parameters	Volume content
Ni ₃ Al + 0.05% B	L1 ₂ , regular orientation Pm3m	0.3566 – 0.3570 ± 0.0002 nm, (theoret. 0.3572 nm) [21]	95.0% and 90.0%
TiB, TiB ₂ 5%	Orthorhombic	a = 0.60630 nm b = 0.30286 nm c = 0.46977 nm (theoret.) [21] a = 0.61050 nm b = 0.30486 nm c = 0.45517 nm	4.2 ± 0.8 (theoret. 5.0%)
TiB, TiB ₂ 10%	Orthorhombic	as above	9.1 ± 0.9 (theoret. 10.0%)

10. Conclusions

The results of the investigation are related with experimental verification of the new methods of fabrication of composites “in situ”, specially the cost-effective process (OPW) of melting NiAlB alloy used as a composite matrix and synthesis (SHSB) of titanium carbides and borides used as a reinforcement of the alloy matrix. Basing on the analysis of the results of the carried out investigation, the following conclusions were formulated:

- Optimal yielding of the intermetallic phase of Ni₃Al is ensured by the addition of boron introduced in an amount of 0.05 wt.%.
- Practical application of the cost-effective melting process (OPW) produced the intermetallic phase Ni₃Al, enriched with an addition of boron (0.05 wt.%) to produce the required structure and chemical composition.
- The SHSB synthesis using titanium-, aluminium- and carbon-containing briquettes produced in alloy matrix (NiAlB alloy) the titanium carbide of a required volume content, phase composition and size of particles. Using this method, Ni₃Al/TiC/5p and Ni₃Al/TiC/10p composites were fabricated.
- The precipitates of TiC particles acting as a reinforcing phase were observed to be distributed within the interdendritic spaces which improved the mechanical and tribological properties.

Acknowledgements

REFERENCES

- [1] A. Janas, Doctor's Thesis. Faculty of Foundry Engineering, Univ. Mining & Metallurgy, (1998) and Research Project of the State Committee of Scientific Research 7TO 8 D 004 09.
- [2] S. Sen, D. M. Stefanescu, B. K. Dhindaw, *Met. and Mat. Trans. A.* **25A**, 2525 (1994).
- [3] J. Barcik, J. Cebulski, *Inżynieria Materiałowa* **1**, 23 (1997).
- [4] J. Barcik, J. Cebulski, *Inżynieria Materiałowa* **4**, 901 (1998).
- [5] S. C. Deevi, V. K. Sikka, *Processing and Applications, Intermetallics*, **4**, 357 (1996).
- [6] C. Liu, C. L. White, J. A. Horton, *Acta Metallurgica* **33**, 1511 (1985).
- [7] F. Dellanay, L. Froyen, *Mat. Science*, **22**, 1 (1987).
- [8] S. Khatri, M. Koczak, *Materials Science Engineering* **A162**, 153 (1993).
- [9] M. Koczak, M. Premkumar, *Journal of Metals* **1**, 41 (1993).
- [10] K. S. Kumar, J. A. Green, L. D. Kramer, *Advanced Materials & Processes*, **4**, 35 (1995).
- [11] G. Tamman, *Anorg. Chem.* **39**, 869 (1926).
- [12] A. G. Merzanov, *Dokl. Akad. Nauk SSSR*, **233**, 430 (1977).
- [13] W. Komatsu, *Proc. 5-th. Intern. Symp. Reactivity of Solids, Monachium*, (1964), Elsevier, Amsterdam, 182.
- [14] J. Dereń, J. Haber, R. Pampuch, *Chemia ciała stałego*, PWN, Warszawa (1975).
- [15] A. Zuhair, Z. Munir, Umberto Anselmi-Tamburini, Elsevier Science Publishers B.V., North-Holland, Amsterdam, 279 (1989).
- [16] Z. Munir, A. Tamburini, *Materials Science Report* **3**, 277 (1989).
- [17] S. C. Deevi, V. K. Sikka, *Intermetallics*, **5**, 17 (1997).
- [18] K. Aoki, J. Izumi, *Japan. Inst. Met.* **43**, 1190 (1979).
- [19] W. Yan, I. P. Jones, R. E. Smalman, *Scripta Metall.* **33**, 1511 (1987).
- [20] S. Wierzbński, T. Czeppe, *Stopy na osnowie faz międzymetalicznych. Scientific Symposium Warsaw 19 October 54* (2000).
- [21] P. Villars, L. D. Calvert, *Pearsons Handbook of Crystallographic Data for Intermetallic Phases USA* **1-4** (1991).

REVIEWED BY: JANUSZ BRASZCZYŃSKI

Received: 20 August 2003.